THE JOURNAL OF BIOLOGICAL CHEMISTRY
Vol. 279, No. 21, Issue of May 21, pp. 22490–22497, 2004

Printed in U.S.A.

Global Co-ordination of Protein Translocation by the SecA IRA1 Switch*

Received for publication, January 29, 2004, and in revised form, March 4, 2004
Published, JBC Papers in Press, March 7, 2004, DOI 10.1074/jbc.M401008200

Eleftheria Vrontou, Spyridoula Karamanou, Catherine Baud, Giorgos Sianidis, and Anastassios Economou‡

From the Institute of Molecular Biology and Biotechnology, Foundation of Research and Technology and Department of Biology, University of Crete, P. O. Box 1527, GR-71110 Iraklio, Crete, Greece

SecA, the dimeric ATPase subunit of protein translocase, contains a DEAD helicase catalytic core that binds to a regulatory C-terminal domain. We now demonstrate that IRA1, a conserved helix-loop-helix structure in the C-domain, controls C-domain conformation through direct interdomain contacts. C-domain conformational changes are transmitted to the DEAD motor and alter its conformation. These interactions establish DEAD motor/C-domain conformational cross-talk that requires a functional IRA1. IRA1-controlled binding/release cycles of the C-domain to the DEAD motor couple this cross-talk to protein translocation chemistries, *i.e.* DEAD motor affinities for ligands (nucleotides, preprotein signal peptides, and SecYEG, the integral membrane component of translocase) and ATP turnover. IRA1-mediated global co-ordination of SecA catalysis is essential for protein translocation.

Bacterial protein translocase comprises the membrane proteins SecYEG, the dimeric peripheral ATPase SecA (1–7), and additional regulatory subunits (8, 9). Secretory proteins associate with SecYEG-bound SecA (5) and activate its ATPase (10). This triggers SecA "insertion-deinsertion" cycles at SecYEG (11, 12) allowing processive translocase movement along the polymeric substrate (13) in defined steps (14).

SecA is built of defined mechanical parts (Fig. 1*A*) (15–19). Each protomer comprises a 68-kDa N-terminal domain (DEAD motor) (16) that is homologous to ATPase domains of DEAD helicases (20). The DEAD motor contains two "RecA-like" subdomains that form a mononucleotide cleft (16, 18, 19, 21): nucleotide binding domain (NBD)[1] (20, 22) and intramolecular regulator of ATPase2 (IRA2) (16). Specificity is provided by two appendages unique to SecA. (*a*) The substrate specificity domain (SSD; Figs. 1 (*A* and *B*) and 5) (17) that contains a globular "bulb" domain and a "stem" that is formed by two anti-parallel β strands (stem "in" and "out") and "sprouts out" of NBD (18, 19). SSD has been implicated in preprotein binding (17, 23, 24). (*b*) The C-domain, fused C-terminally to IRA2, participates in SecA dimerization (15, 25) and contains four substructures (Fig. 1*A*) (18, 19): the scaffold domain (SD), a 46-aa-long bent α-helix, which docks the C-domain to the DEAD motor by acting as a molecular staple binding both NBD and IRA2; the flexible wing domain (WD); IRA1 (15), a conserved helix-loop-helix (H1-L-H2) that fits between SD and SSD (Fig. 5); and the extreme C-terminal region (CTD), which is largely crystallographically unresolved and binds lipid and SecB (26, 27).

Energy conversion to mechanical work remains a central unresolved issue in several DEAD helicases (20, 21, 28) as well as in protein translocation. The mechanism is expected to involve cross-talk between the ATP motor and specificity domains (13, 16, 17). In SecA, evidence for this is provided by the finding that, in the absence of tight C-domain association, the DEAD motor becomes a hyperactivated ATPase (15, 18, 19). Importantly, SecA with a short IRA1 deletion also becomes an unregulated, hyperactivated ATPase that is nevertheless incompetent for translocation (15). This observation led us to propose that IRA1 is a molecular switch essential for coupling ATP hydrolysis to translocation work (15). We now show that IRA1 contacts other SecA subdomains and through these it controls association and conformational cross-talk between the DEAD motor and the C-domain. Modulation of these physical contacts allows IRA1 to regulate DEAD motor subactivities. We propose that SecA ATP binding and hydrolysis become coupled to protein translocation through IRA1 acting as a global co-ordinator of translocase catalysis and conformation.

MATERIALS AND METHODS

Bacterial Strains and Recombinant DNA Experiments—Escherichia coli strains were grown and manipulated as described (15, 16, 29). IRA1 mutations were constructed on pIMBB38 (*secA* in BamHI-EcoRI sites of pALTER-EX1) using Altered sites (Promega) using primers: X61 (CAGGTGCTCTTTCGCCAGGGAGTCAAG; W775A), X62 (GATACCCTGACGCCGATAGTCCATCGC; L785R), X63 (GCCACGCAGGTGGCGACCCTGACGCAG; I789R), X64 (CTGTGCGTAGCCAGCCAGGTGGATACC; R792A), X65 (GTATTCCTGCTTCGCATCTTTCTGTGC; P799A), X66 (TTCACGTTTGTATGCCTGCTTCGGATC; E802A), X67 (CGATTCACGTTTGGCTTCCTGCTTCGG; Y803A), X68 (CATGGAGAACGATGCACGTTTGTATTC; E806A), and X69 (CAGCATCGCTGCAGCCATGGAGAACGA; F811A). Next, the 2.9-kb NcoI fragment of pIMBB7 (HisSecA) was replaced by that of mutant genes, giving rise to pIMBB105, pIMBB106, pIMBB202, pIMBB107, pIMBB200, pIMBB108, pIMBB109, pIMBB110, and pIMBB201, respectively.

The 0.83-kb EcoRI-MfeI fragment of *secA* IRA1 mutants was also cloned into the corresponding sites of pIMBB70 (HisC34) giving rise to pIMBB165, pIMBB166, pIMBB167, pIMBB168, pIMBB169, pIMBB181, pIMBB182, pIMBB183, and pIMBB184, respectively.

C34 truncations were constructed by PCR, using pIMBB70 as template. For C609–834 and C669–834, we used forward primers X110 (GGCCCGTACATATGAAACTGGGTATGAAGCCAGGC) and X109 (GGCCCGTACATATGGTCAGCGATGTGAGCGAAACC), respectively, and the reverse

* This work was supported by European Union Grants TMR-ERBFMRXCT960035, Biotech2-BIO4-CT98-0051, RTN1-1999-00149, QLK3-CT-2000-00082, and QLRT-2000-00122 and by a grant from Pfizer, Inc. The costs of publication of this article were defrayed in part by the payment of page charges. This article must therefore be hereby marked "*advertisement*" in accordance with 18 U.S.C. Section 1734 solely to indicate this fact.

This paper is dedicated to the memory of Bob Macnab.

‡ To whom correspondence should be addressed. Tel./Fax: 30-2810-391166; E-mail: aeconomo@imbb.forth.gr.

[1] The abbreviations used are: NBD, nucleotide binding domain; MANT, 2′(or 3′)-*O*-(*N*-methylanthraniloyl)adenosine 5′-diphosphate; SSD, substrate specificity domain; SD, scaffold domain; CTD, extreme C-terminal domain; WD, wing domain; BSA, bovine serum albumin; IRA, intramolecular regulator of ATPase; aa, amino acid(s); IMV, inner membrane vesicle.

primer X107 (CGCGGATCCTTAAGGCATACGTACCTGAACTTTG). For C609–757, we used forward primer X110 (GGCCCGTACATATGAAACTGGGTATGAAGCCAGGC) and reverse primer X111 (CGCGGATCCTTACTCAGCACCAACCACTTCTTC). PCR fragments were digested with NdeI/BamHI and inserted into pET16b (Invitrogen), resulting in pIMBB203, pIMBB186, and pIMBB185, respectively.

ATP Hydrolysis Measurements—All assays were in buffer B (50 mM Tris-Cl, pH 8, 50 mM KCl, 5 mM $MgCl_2$, 1 mM dithiothreitol), 1 mg/ml BSA, 1 mM ATP. SecA or N68 derivatives were added at 0.1 mg/ml. For membrane ATPase SecYEG-proteoliposomes (200 μg/ml) were added. For translocation ATPase proOmpA (0.2 mg/ml) was further added. For N68 suppression assays C34 derivatives were added as indicated in figure legends. Released phosphate was measured using malachite green detection (10) or using thin layer chromatography (TLC). For TLC [γ-^{32}P]ATP was mixed with ATP to a final concentration of 20–1000 μM (16). K_{cat} values were determined as described (16) using Prism 4.0 (GraphPad).

Fluorescence Measurements—Measurements were carried out in quartz cuvettes (1 ml; Hellma) with a Cary Eclipse fluorimeter supplemented with a four-position cuvette holder and a Peltier temperature controller (Varian). For determination of equilibrium dissociation constants, SecA was added at increasing concentrations (0.025–5 μM) to MANT-ADP (0.1 μM; Molecular Probes) in buffer B. Emission spectra of MANT-ADP were recorded at each step of the binding curve (380–550 nm; excitation 356 nm; slits at 2.5 and 20 nm). K_D was determined by plotting the change of MANT-ADP emission spectra upon SecA addition against SecA concentration using the equation $(F_1 - F_0)/F_0$ integral values (F_0 = no SecA added, F_1 = SecA added). To determine apparent T_m, we monitored changes in intrinsic tryptophan fluorescence emission of SecA or C34 derivatives (0.25 μM in buffer B) as a function of increasing temperature (4–82 °C; ramping rate 0.8 °C/min; excitation 297 nm/emission 345 nm; slits at 2.5 and 20 nm; data acquisition interval = 0.5 min), in the presence or absence of ADP (2 mM). All data were collected using Cary Eclipse software (Bio Package; Varian) and analyzed by nonlinear regression using Origin 5.0 (Microcal).

Surface Plasmon Resonance Assays—Optical biosensor measurements were on an IBIS II instrument (Echochemie). 3K7L (3 μg in 50 μl from a 60 μg/ml stock in 10 mM Hepes, pH 8.5) was added onto carboxymethylated dextran-coated gold sensor disks (CMD20; Xantec) and was cross-linked via NH_2-specific *N*-ethyl-*N*′-(dimethylaminopropyl)-carbodiimide/*N*-hydroxysuccinimide. The surface was regenerated with 100 mM HCl. Data were collected (750 s) and analyzed using IBIS Kinetic Analysis software (17).

SecA Binding to SecYEG—Binding of ^{35}S-labeled SecA proteins to inner membrane vesicles (IMVs) was performed as described elsewhere (5). Briefly, urea-treated IMVs (64 μg/ml) were mixed with a range of ^{35}S-labeled SecA concentrations (0.5–2000 nM; buffer B; 1 mg/ml BSA; 15 min; 4 °C). Reactions were overlaid on equal volume of buffer B, 0.2 M sucrose, 1 mg/ml BSA, in centrifuge tubes preblocked with BSA and sedimented (320,000 × *g*; 30 min; 4 °C; Beckman TLX120 ultracentrifuge). Pellets, rinsed (two times; 100 μl of buffer B) and resuspended by sonication, were spotted on nylon membranes in a vacuum manifold (Bio-Rad). Bound radioactivity was quantitated by phosphorimaging. Data were fitted to hyperbolae using nonlinear regression in Prism (GraphPad).

Chemicals and Biochemicals—Proteases, inhibitors and nucleotides were from Roche; *E. coli* phospholipids were from Avanti Polar Lipids; DNA enzymes from Minotech; oligonucleotides from MWG; dNTPs from Promega; [γ-^{32}P]ATP (5000 Ci/mmol), [^{35}S]methionine (1000 Ci/mmol), and chromatography materials (except Ni^{2+} affinity; Qiagen) from Amersham Biosciences; all other chemicals from Sigma. Biochemicals were purified as described elsewhere (6, 10, 15, 16).

Miscellaneous—Protein concentration was determined using the Bradford reagent (Bio-Rad) with BSA as a standard or by UV absorbance or by amino acid analysis. Biochemical assays, trypsinolysis experiments, preparation of SecYEG inner membrane vesicles and proteoliposomes, sodium dodecyl sulfate-polyacrylamide gel electrophoresis (SDS-PAGE), ^{35}S-labeled SecA binding to IMVs, and SecA reconstitution from N68 and C34 were as described (5, 15–17). CD spectroscopy assays were performed as described previously (15). Native PAGE was carried out using a Bio-Rad Mini-PROTEAN II system. α-NBD and α-IRA2 rabbit polyclonal antibodies were raised against purified N1–263 and N462–610, respectively. α-SSD antibodies were purified as described (17). Radioactivity was quantitated by phosphorimaging (Storm 840; Amersham Biosciences). N-terminal sequencing and amino acid analysis were done at AltaBioscience (United Kingdom). Structures were analyzed with SwissPDBViewer.

RESULTS

IRA1 Mutations Compromise SecA-mediated Protein Translocation—To understand IRA1 function, we mutated its nine most highly conserved residues (Figs. 1 (*A* and *B*) and 5) (15, 16). The ability of IRA1 mutants to complement the chromosomal thermosensitive *secA* gene of strain BL21.19 (15, 29) was examined (Fig. 1*C*). Six of the mutants (*secAL785R*, *secAI789R*, *secAP799A*, *secAE802A*, *secAY803A*, and *secAE806A*) were barely viable, as was partial deletion of IRA1 (*secA*Δ783–795) (15, 30). Three mutants (*secAW775A*, *secAF811A*, and *secAR792A*) complemented the thermosensitive strain, albeit not as efficiently as *secA*.

Oligohistidinyl-tagged SecA IRA1 mutants were purified and shown, like SecAΔ783–795 (15, 30), to be stable, folded, and α-helical (far UV CD; data not shown) and dimeric (size exclusion chromatography, blue native PAGE, sedimentation equilibrium; data not shown). We concluded that IRA1 mutant proteins do not have significantly altered structures and were characterized biochemically.

To verify that the *in vivo* phenotypes (Fig. 1*C*) are the result of defective protein export, HisSecA IRA1 mutants were used in an *in vitro* translocation assay with SecYEG-proteoliposomes and the secretory protein proOmpA (Fig. 1*D*) (6). Of all IRA1 mutants, only SecAW775A (*lane 5*) supports protein translocation (*lanes 6–13*). SecAR792A (*lane 8*) and SecAF811A (*lane 13*) do not translocate *in vitro*, although they partially complement *in vivo* (Fig. 1*C*). Clearly, the more stringent and suboptimal *in vitro* proteoliposome assay exacerbates their defects.

IRA1 Mutations Alter SecA ATPase Activities—To test whether IRA1 mutants are defective in ATP catalysis, we determined their basal, membrane, and translocation ATPase activities (Table I). Basal ATP catalysis is enhanced, either significantly (>13-fold; SecAW775A; >5-fold SecAF811A) or slightly (up to 2-fold; all other mutants except SecAI789R). Stimulation of basal ATPase upon addition of SecYEG-proteoliposomes (membrane ATPase) or proteoliposomes plus proOmpA (translocation ATPase) is seen only with SecAW775A, SecAR792A, and SecAF811A in agreement with the *in vivo* complementation test (Fig. 1*C*). All other IRA1 mutant proteins fail to further stimulate their basal ATPase.

Based on the above results, IRA1 mutants fall into three classes: (i) the functional/hyperactivated W775A, (ii) the less-functional R792A and F811A, and (iii) the severely compromised L785R, I789R, P799A, E802A, Y803A, and E806A. To simplify presentation we will focus hereafter on three representative mutants: SecAW775A, SecAR792A, and SecAI789R.

IRA1 Mutations Alter SecA Affinity for Nucleotide—To understand how IRA1 influences SecA ATP catalysis, we examined the effect of IRA1 single point mutations or partial deletion on nucleotide binding to SecA. To this end we developed a fluorescent MANT-ADP binding assay (Table II).

At 4 °C, MANT-ADP binds to SecA with high affinity (K_D = 0.14 μM). This is in agreement with values obtained with other methods (29, 31). N68, the polypeptide carrying the complete DEAD motor bereft of the C-domain (15), exhibits similarly high affinity (K_D = 0.28 μM). C34, the polypeptide carrying the C-domain alone (15), has no measurable nucleotide binding (data not shown). In agreement with biochemical (16) and structural analysis (18, 19), these data demonstrate that the DEAD motor domain of SecA is necessary and sufficient for nucleotide binding.

Temperature does not affect nucleotide binding to the DEAD motor in SecA (37 °C; Table II). In contrast, it drastically reduces binding to the isolated DEAD motor (>350-fold). This suggests that the C-domain acts in *trans* to determine DEAD

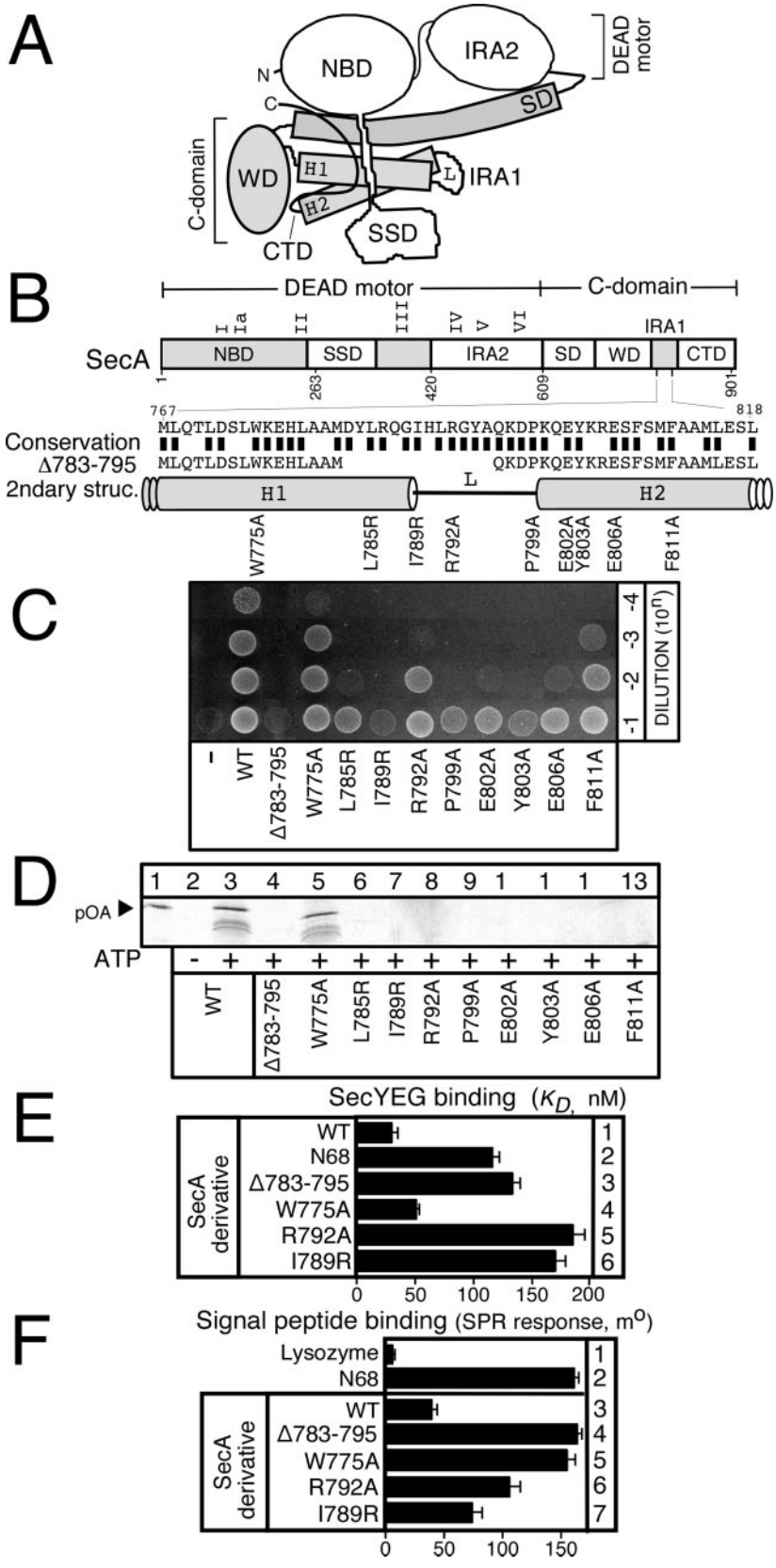

FIG. 1. **IRA1 mutational analysis.** *A*, model of SecA protomer (15–19). *B*, SecA schematic. *Latin numerals*, DEAD family motifs (16, 20). A partial map (aa 767–818) of IRA1 is shown with conserved residues (>70% identity; *black bars*) (16). Point mutations are indicated *below* the secondary structure map: *cylinders*, α-helices; *L*, loop. *C*, genetic complementation of IRA1 mutants. BL21.19 cells carrying pET5 vector alone or with cloned *secA* IRA1mutations were grown at 30 °C (12 h; Luria broth). Indicated dilutions were spotted on Luria-Bertani broth/ampicillin plates and incubated at 42 °C. *D*, *in vitro* ATP-driven protein translocation of [^{35}S]proOmpA (60,000 cpm/μl) into SecYEG-proteoliposomes (200 μg/ml) catalyzed by SecA (*lane 3*) or IRA1derivatives (*lanes 4–13*). *Lane 1*, 25% of input [^{35}S]-proOmpA; *lane 2*, minus ATP control. *E*, dissociation constants of SecA and derivatives for SecYEG (70 μg/ml IMVs, 4 °C, buffer B) determined as described elsewhere (5). *F*, equilibrium binding of SecA, N68, or SecA IRA1 derivatives (2 μM) to a signal peptide biosensor (17). *Lane 1*, lysozyme negative control.

motor nucleotide affinity at physiological temperature. Partial deletion or single point mutations in IRA1 reduce SecA nucleotide affinity, suggesting that IRA1 may be part of this mechanism.

IRA1 Mutations Alter SecA Affinity for SecYEG—Because membranes do not stimulate the ATPase of most IRA1 mutants (Table I), their binding to SecYEG might be defective. To investigate this we determined the equilibrium dissociation constants of SecA IRA1 derivatives for SecYEG (Fig. 1*E*).

SecA binds to SecYEG in IMVs with high affinity (K_D = 30 nM; *lane 1*) (5). N68 binding to SecYEG is 4-fold reduced (K_D = 110 nM; *lane 2*), whereas no C34 binding was measurable (data

TABLE I
Steady state ATPase kinetic constants of SecA IRA1 mutants

SecA derivative	K_{cat}		
	Basal	Membrane	Translocation
		min^{-1}	
WT	3.7 (±0.4)	6.2 (±0.6)	25 (±6)
Δ783–795	45 (±6)	43 (±7)	43.2 (±7)
W775A	50.4 (±7)	54 (±10)	76 (±13)
L785R	5.7 (±0.6)	4.6 (±0.4)	6.8 (±0.7)
I789R	3 (±0.3)	3 (±0.3)	2.6 (±0.2)
R792A	4.3 (±0.4)	16 (±2.5)	24.7 (±5)
P799A	5.2 (±0.5)	3.2 (±0.3)	9 (±1)
E802A	5.5 (±0.5)	5.7 (±0.4)	7.4 (±0.6)
Y803A	8.4 (±0.6)	7.3 (±0.6)	7 (±0.5)
E806A	4.1 (±0.3)	1.3 (±0.2)	5.4 (±0.4)
F811A	18.7 (±4)	32 (±7)	54 (±11)

TABLE II
Equillibrium dissociation constants of SecA and derivatives for MANT-ADP, at the indicated temperature
Triplicates of 40–60 data points were used for each binding curve.

SecA derivative	K_{Di}	
	4 °C	37 °C
	μM	
SecA	0.14 (±0.02)	0.28 (±0.03)
N68	0.28 (±0.03)	>100
Δ783–795	0.75 (±0.1)	8.18 (±2.5)
W775A	0.17 (±0.04)	4.58 (±1.1)
R792A	0.4 (±0.08)	0.38 (±0.02)
I789R	1.02 (±0.19)	0.7 (±0.07)

not shown) (32). These data indicate that SecA binds to SecYEG through the DEAD motor, but the presence of the C-domain optimizes binding affinity. This C-domain contribution requires an intact IRA1 because partial deletion or single point mutations in IRA1 reduce SecA DEAD motor affinity for SecYEG (Fig. 1*E*).

IRA1 Mutations Alter Signal Peptide Binding to SecA—We next examined the ability of IRA1 mutants to interact with preprotein signal peptides (Fig. 1*F*). SecA (*lane 3*), but not an unrelated control protein (*lane 1*), binds to a signal peptide (3K7L) biosensor (17, 33). The DEAD motor of SecA is necessary and sufficient for signal peptide binding (*lane 2*) (17). The presence of the C-domain in SecA prevents maximal signal peptide binding to the DEAD motor (compare *lanes 3* and *2*) (17). IRA1 mutations seem to overcome this and render the SecA DEAD motor more competent for signal peptide binding (compare *lane 3* with *lanes 4–7*).

IRA1 Mutants Exhibit Altered DEAD Motor Conformation—SecA DEAD motor chemistries are affected by the absence of the C-domain or by mutations in IRA1 (Tables I and II and Fig. 1, *E* and *F*). This effect could reflect alteration of DEAD motor conformation. To investigate this we developed an assay that monitors DEAD motor conformation in SecA IRA1 mutants using limited trypsinolysis (15), followed by immunostaining with domain-specific antibodies (α-NBD, α-IRA2, and α-SSD; Fig. 2).

Despite the fact that the overall structure and organization of SecA IRA1 mutants is undisturbed, changes in the tryptic profile of the mutants were detectable. Cleavage of the DEAD motor (p67 peptide; *panel A*, *lane 2*) appears more rapid in IRA1 mutants and occurs within the NBD-IRA2 linker (aa 420; *panels A*-C), within IRA2 (aa 561 and 585; *panel B*), within NBD (aa 201; *panel C*), at the base of the SSD $stem_{out}$ (aa 220; *panel C*) and within the SSD bulb (aa 360; *panel C*). The DEAD motor of SecAI789R seems particularly sensitive to trypsinolysis (*panel A*, *lane 5*) and gives rise to slightly different IRA2 and SSD peptides (*panels B* and *C*, *lane 5*).

Most of these tryptic sites become inaccessible when ADP is pre-bound to SecA (compare *lane 6* with *lane 2*; aa 220, 420, and 561) (15, 17). IRA1 mutants can acquire the "ADP-bound state" characterized by enhanced p67 stability (*lanes 6–9*). However, this conversion is less efficient than in SecA because some cleavage still occurs (*lanes 7–9*; *panels B* (aa 420 and 561) and *C* (aa 221)). None of the DEAD motor tryptic sites is in immediate contact with IRA1 (*panel D*) (18, 19), and yet cleavage is affected by IRA1 mutations, suggesting that they may cause long range conformational effects.

Next we probed the effect of IRA1 mutations on DEAD motor conformation by a different method, thermal melting monitored by far UV CD. In this assay, SecA and N68 melt in two distinct steps ($T_{m1(app)}$ and $T_{m2(app)}$) that represent loss of secondary structure within the DEAD motor (Table III) (16). Both of the SecA $T_{m(app)}$ are stabilized significantly by ADP, whereas only $T_{m2(app)}$ is stabilized in N68 (Table III) (16). SecA IRA1 mutants also display two melting transitions, indicating that their DEAD motors are structurally similar to that of SecA (Table III). Nevertheless, their $T_{m(app)}$ are altered.

DEAD Motor Affects C-domain Conformation—IRA1 mutations affect DEAD motor conformation (Fig. 3, *A–C*). To test whether the DEAD motor can reciprocally affect C-domain conformation, we monitored SecA intrinsic Trp fluorescence during thermal melting. This assay specifically follows C-domain conformation because its three Trp residues (aa 701, 723, and 775) are the main contributors of SecA fluorescence (18–34). The derived $T_{m(app)}$ is unrelated to those obtained by CD (see above).

Under these conditions SecA displays a characteristic $T_{m(app)}$ (43 °C) that is significantly stabilized by ADP (48 °C; Fig. 2*E*) (18). Clearly, the ADP-induced conformational change of the DEAD motor (Table III) (16, 35) is transmitted at a distance and sensed by C-domain tryptophans (18–35). IRA2 mutations that compromise DEAD motor conformation (G510A) or nucleotide binding (R577K) (Figs. 1*B* and 2*D*; Ref. 16) interfere with DEAD motor/C-domain conformational cross-talk because they lead to $T_{m(app)}$ changes in the absence or presence of ADP (Fig. 2*E*). SecAW775A and SecAR792A, which exhibit practically wild type $T_{m(app)}$ in the apoprotein state, fail to acquire specifically the ADP-induced C-domain conformation of SecA (Fig. 2*E*). SecAI789R exhibits a lower $T_{m(app)}$ than SecA, even in the absence of ADP.

Our results indicate that there is conformational cross-talk between the DEAD motor and the C-domain, and this requires a functional IRA1.

IRA1 Mutations Affect DEAD Motor/C-domain Assembly—Interdomain conformational cross-talk in SecA (Fig. 2; Table III) is presumably mediated through physical contact. Because partial IRA1 deletion abolishes DEAD motor/C-domain physical association (15), IRA1 might modulate this association. To

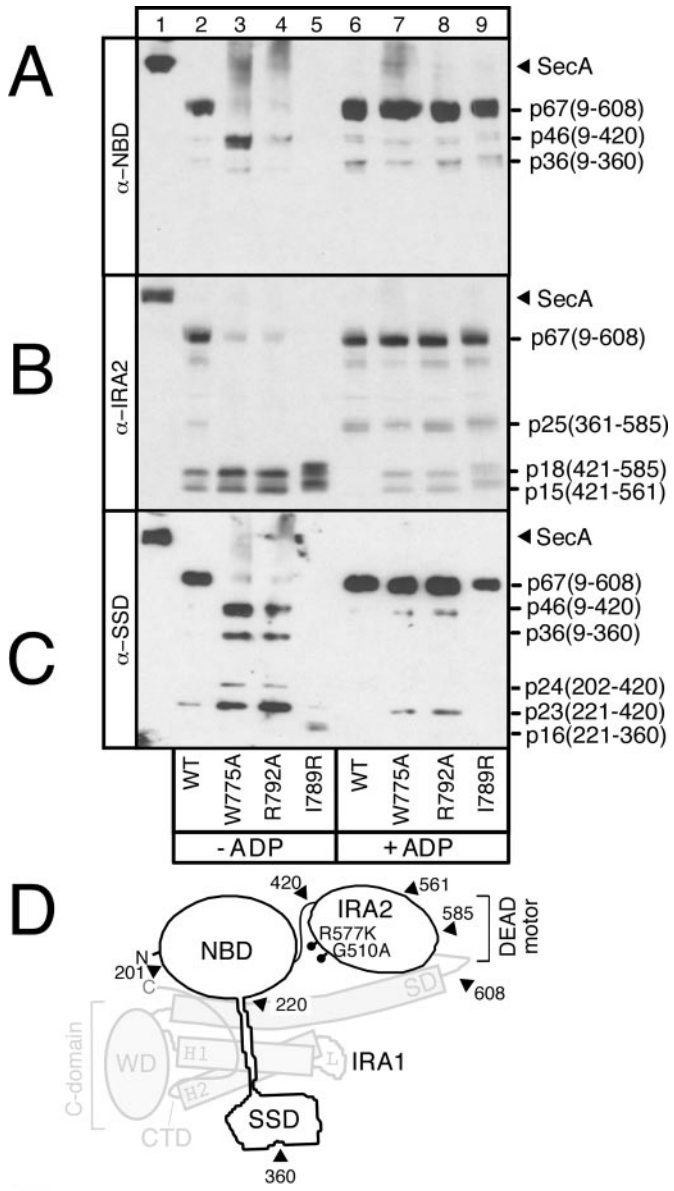

	*Tm*app	
	- ADP	+ ADP
WT	43	48
G510A	35.2 + 43	44
R577K	43.5	46
W775A	43	45.5
R792A	43	47
I789R	40.6	46.7

FIG. 2. **Effect of IRA1 mutations on DEAD motor and C-domain conformations.** *A–C*, limited trypsinolysis (0.025 mg/ml trypsin, 13 min, 4 °C) of SecA and indicated IRA1 mutants (0.3 mg/ml; buffer B), in the absence or presence of ADP (1 mM) as in Ref. 15. Polypeptides were analyzed by 17% 6 M urea SDS-PAGE gels and stained with α-NBD (*A*), α-IRA2 (*B*), or α-SSD (*C*) antibodies. Peptides were identified by N-terminal sequencing. *D*, SecA model with DEAD motor tryptic sites (*panels A–C*) and IRA2 mutations. *E*, $T_{m(app)}$ of SecA and derivatives (0.25 μM; buffer B), determined from fluorescence spectra acquired as a function of temperature. $n = 4$.

test this we examined the ability of HisC34 derivatives to bind to N68 by native PAGE (Fig. 3A). Successful C34/N68 association generates a novel electrophoretic species that migrates slower than the individual domains (*lane 4*) (15) and is similar to that of native dimeric SecA (*lane 1*). Formation of this

TABLE III
Apparent T_m of SecA and derivatives

Ellipticity at 222 nm was monitored by far UV CD spectra during thermal melting (15).

Polypeptide	$T_{m1(app)}$		$T_{m2(app)}$	
	−ADP	+ADP	−ADP	+ADP
SecA	39.6	44.9	48.9	58.0
N68	39.2	39.6	48.5	58.0
SecAW775A	38.8	42.0	49.5	51.4
SecAR792A	37.9	45.4	45.5	56.0
SecAI789R	34.3	39.6	49.2	54.1

complex is clearly affected by some IRA1 mutations. Samples containing C34W775A (*lane 6*) or C34F811A or C34Y803 (data not shown) migrate as fuzzy bands suggesting that these mutant C-domains fail to form tight complexes with N68. Other mutants form reconstituted complexes of the expected size in slightly (5–20%) reduced amounts (*lanes 8* and *10*). Successful C34 binding to N68 suppresses its elevated ATPase (Fig. 3*B*, *lane 1*) (15). As expected, C34W775A, which fails to form stable physical complexes (Fig. 3*A*, *lane 6*), cannot suppress N68 ATPase (Fig. 3*B*, *lane 2*). Interestingly, DEAD motor ATPase suppression by C34R792A (*lane 3*) and C34I789R (*lane 4*), which form physical complexes (Fig. 3*A*, *lanes 8* and *10*), is inefficient.

Taken together, our data suggest that IRA1 has a crucial role in physical and/or functional C-domain/DEAD motor assembly.

IRA1 Is Required for Scaffold Domain Binding to the DEAD Motor—SD is the only C-domain substructure that binds to the DEAD motor (18, 19). Then why do IRA1 mutations affect this association (Fig. 3)? (15) To understand this we generated three truncated C34 derivatives (Fig. 3*C*) and examined their binding to N68 by native PAGE (Fig. 3*D*). C609–834 (devoid of CTD) binds to N68 (compare *lane 5* with *2*) but neither C609–757 (IRA1 deleted; *lane 3*) nor C669–834 (SD deleted; *lane 4*) do. In accordance, only C34 (Fig. 3*E*, *lane 1*) and C609–834 (*lane 4*; SD plus WD plus IRA1) functionally suppress DEAD motor ATPase, whereas C609–757 (*lane 2*) and C669–834 (*lane 3*) cannot.

Our results suggest that the concomitant presence of both IRA1 and SD is required for SD binding to the DEAD motor.

IRA1 Mutations Affect C-domain Conformation—To explain how IRA1 influences SD binding to the DEAD motor, we hypothesized that IRA1 may affect SD conformation (Figs. 2*E* and 3). We therefore examined the effect of IRA1 mutations on C-domain conformation by limited trypsinolysis (Fig. 4*A*) and intrinsic Trp fluorescence (Fig. 4, *B* and *C*).

Trypsin cleaves C34 within SD, at Lys-643, giving rise to p30 (Fig. 4*A*, *lane 2*). p30 is then cleaved within CTD, giving rise to p28 and to small peptides (*lane 2*). C34 IRA1 mutants display either more rapid proteolysis of p30 and p28 (*e.g.* W775A; *lane 3*) or enhanced resistance of p30 and p28 (*e.g.* R792A; *lane 4*) or delayed cleavage at Lys-643 (*e.g.* I789R; *lane 5*). We additionally observed that C34E802A undergoes cleavage within SD, at Lys-643, from an unknown cellular protease during purification, and the resulting polypeptide remains stable thereafter (data not shown). These results indicate that mutations in IRA1 affect the conformation of both SD and CTD, where the tryptic sites are located.

We further monitored the conformation of C34 IRA1 mutants by Trp fluorescence during thermal melting (Fig. 4*B*). This assay follows conformational changes specifically sensed by Trp-701/Trp-723 in WD (18, 34) because Trp-775 only contributes to the total Trp emission of C34 (compare C34 with C34W775A; *panel C*) but not to the measured C34 $T_{m(app)}$ (*panel B*). C609–834 and C669–834 maintain the $T_{m(app)}$ of C34, indicating that CTD or SD either do not significantly

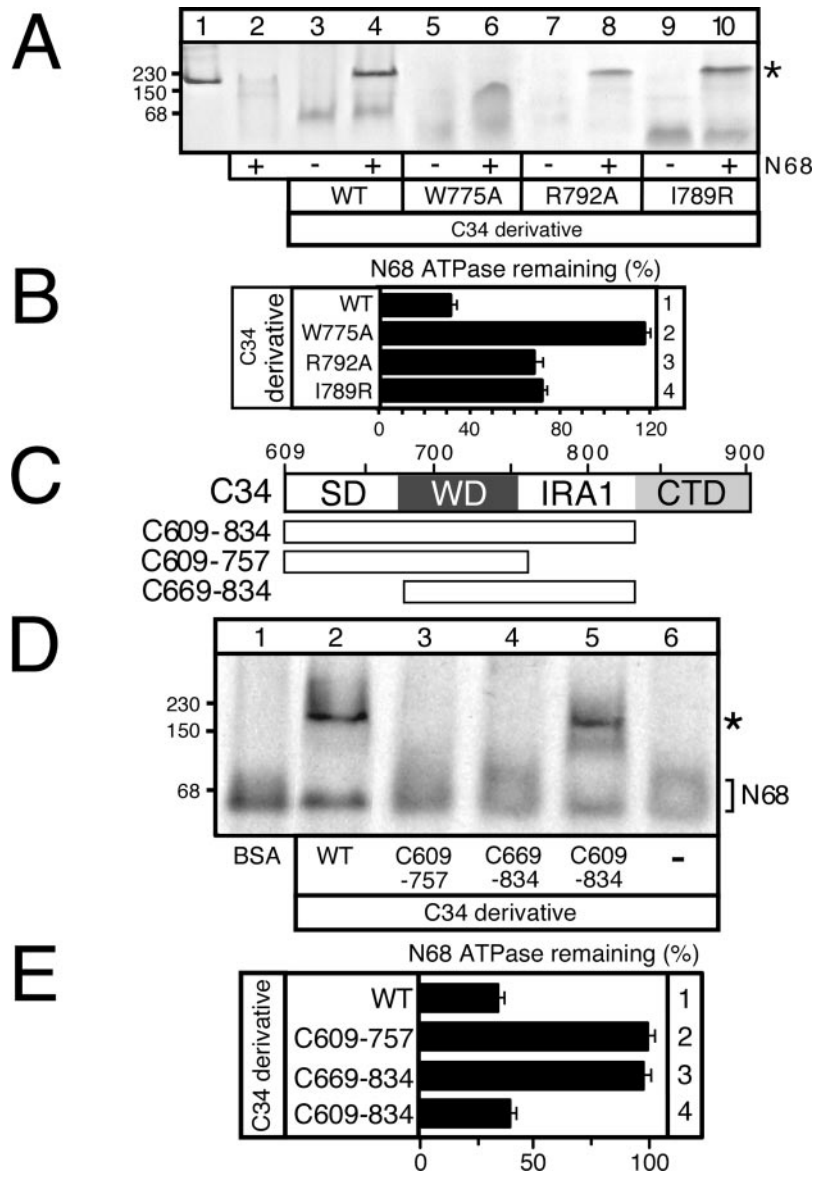

FIG. 3. **C-domain/DEAD motor interaction requires IRA1.** *A*, physical reconstitution (30 min; 4 °C; buffer B) (15) of SecA dimers (*) from purified N68 (3 μg) and 12 molar excess C34 IRA1 mutants. Complexes were analyzed by 10% native-PAGE and stained with Coomassie Blue. *Lane 1*, SecA (204 kDa). Molecular size standards were catalase (230 kDa), aldolase (150 kDa), and BSA (68 kDa). *B*, N68 ATPase (100%) suppression by C34 IRA1 mutants. Remaining ATPase of samples (*lanes 2–10*) in *A* was measured and C34 background subtracted. *C*, map of C34 truncations. *D*, N68/C34 truncation physical association. [^{35}S]N68 (2 μl; 100,000 cpm) was mixed with 5 μM C34 or C609–757 or C669–834 or C609–834 or BSA and incubated (30 min; 4 °C; buffer B). Polypeptides were analyzed as in *A* and visualized by phosphorimaging. *, N68/C34 complex. MW standards as in *A*. *E*, N68 ATPase suppression by C34 truncations. C34 (*lane 1*) or C34 truncations (*lanes 2–4*) were added to N68 as in *A* and analyzed as in *B*.

contribute to C-domain conformation or that their deletion is not "sensed" by the WD (*panel B*). In contrast, partial or complete IRA1 deletion leads to significantly increased $T_{m(app)}$ (compare C34 to C34Δ783–795 and C609–757), suggesting that IRA1 mutations affect WD conformation.

Finally, IRA1 mutations that do not remove any Trp residue affect C34 total Trp emission (*e.g.* R792A and I789R; Fig. 4*C*) and/or $T_{m(app)}$, suggesting the occurrence of a conformational change that alters emission from the same Trp residues. An extreme case is C34E802A; emission is virtually abolished (*panel C*), although cleavage during purification (see above) does not remove any of the emitting Trp residues.

Our data suggest that IRA1 mutations affect C-domain conformation *in toto*.

DISCUSSION

The DEAD motor, the catalytic core of SecA, is necessary and sufficient for nucleotide binding (Table II) and hydrolysis (Table I), signal peptide binding (Fig. 1*F*) (17, 36), and SecYEG binding (Fig. 1*F*) (32). The structurally independent and juxtaposed C-domain binds to the DEAD motor and suppresses its ATPase (Fig. 3*B*) (15). We now show that the C-domain determines DEAD motor ligand binding affinities (Fig. 1 (*E* and *F*) and Table II) and catalysis (Table I) in *trans*. This regulation requires specifically IRA1, a conserved C-domain substructure. IRA1 mutations or partial deletion cause measurable alterations in all DEAD motor chemistries (Tables I and II; Fig. 1, *E* and *F*) that lead to defective protein translocation (Fig. 1, *C* and *D*).

IRA1 has a characteristic hairpin structure formed of intersecting helices (Figs. 1 (*A* and *B*) and 5 (*A* and *B*)). These assemble through highly conserved, mainly hydrophobic, residues that include the ones mutated here: Leu-785 and Ile-789 on H1, Tyr-803 on H2, and Pro-799 that defines a sharp H2-L boundary. Local deformation of the hairpin structure might prevent/alter H1/H2 relative movement. Such motion is common in other proteins with H-L-H structures such as calmodulin (37) and may be essential for IRA1 function. Mutation or deletion of these residues severely compromises SecA function (Fig. 1*C*), as does a three-residue insertion after Pro-799 (15). Clearly, IRA1 structural integrity is crucial for SecA function. Contact to the second protomer, as suggested by the *B. subtilis* crystallographic dimer (18), might additionally stabilize the IRA1 hairpin structure. Mutation of Glu-802 that mediates such an interaction leads to a severely compromised mutant (Fig. 1 (*C* and *D*); Table I). Our data indicate that the presence of the IRA1 hairpin destabilizes the C-domain (Fig. 4*B*) and

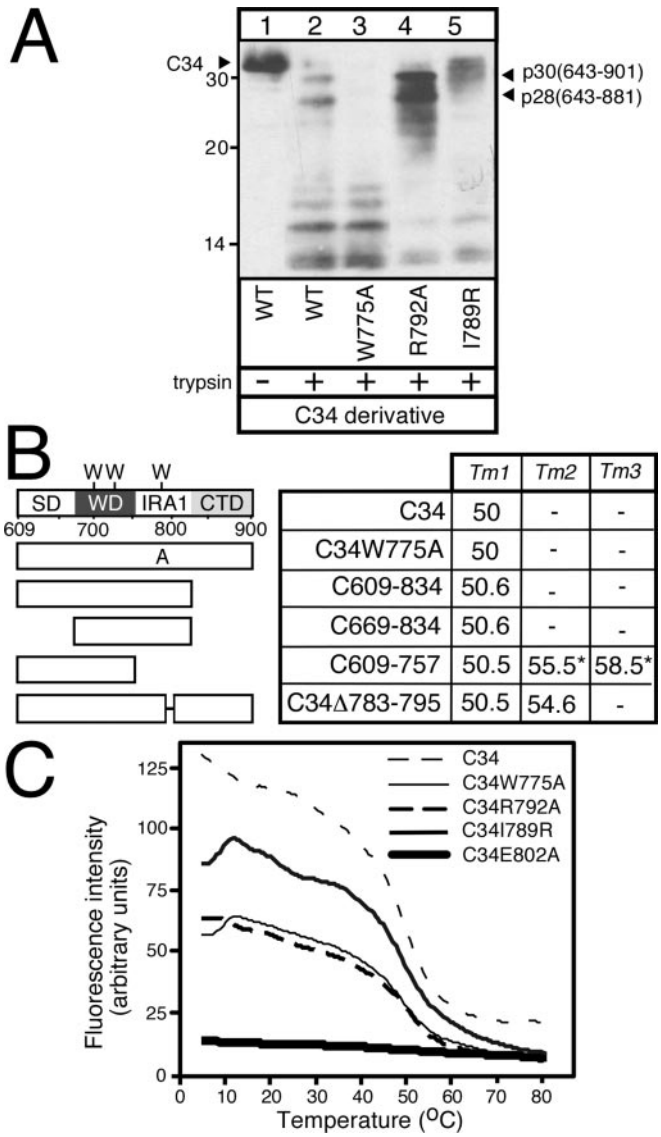

	Tm1	Tm2	Tm3
C34	50	-	-
C34W775A	50	-	-
C609-834	50.6	-	-
C669-834	50.6	-	-
C609-757	50.5	55.5*	58.5*
C34Δ783-795	50.5	54.6	-

FIG. 4. **IRA1 regulates C-domain conformation.** *A*, Limited trypsinolysis (0.25 mg/ml; 5 min; 4 °C) of C34 and IRA1 derivatives (0.3 mg/ml). Samples were analyzed as in Fig. 2 and silver-stained. *Lane 1*, undigested C34. *B*, $T_{m(app)}$ of C34 derivatives (0.25 μM; in buffer B) determined as in Fig. 2*E*. On the schematic *W* is fluorescence-emitting Trp residues (18, 35). *, main $T_{m(app)}$. $n = 4$. *C*, Trp fluorescence emission spectra of C34 and derivatives upon thermal melting.

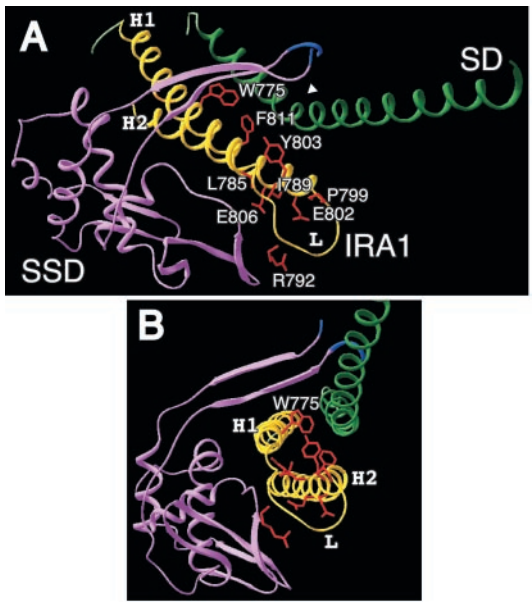

FIG. 5. **Mutated IRA1 residues (*red*) in the SecA structure (see text for details).** Figure shows data from *B. subtilis* SecA (Protein Data Bank code 1M6N (see Ref. 18)). *A*, top-side and B, front view. *White arrow*, SD α-helix bent. *Blue*, residues connecting to NBD.

that mutations in IRA1 affect the conformation of all other C-domain subdomains (Fig. 4, *A* and *C*), suggesting that IRA1 is important for C-domain flexibility (38).

IRA1 is not a structural component of the DEAD motor (Fig. 1*A*) and makes no direct contacts with either NBD or IRA2 (18, 19). How then does IRA1 affect DEAD motor chemistries? The IRA1 hairpin seems strategically positioned in the SecA structure; IRA1 H1 fits in a spacious three-sided enclave formed by SD, SSD, and WD and "capped" only by the stem of SSD, whereas the IRA1 loop and most of IRA1 H2 are completely solvent-exposed (Fig. 5, *A* and *B*). Through conserved outwardly facing residues, the IRA1 hairpin makes two main crucial contacts with surrounding subdomains (Figs. 1*A* and 5 (*A* and *B*). (*a*) The first is IRA1-SD; this is a tight interaction mediated by two bulky aromatic residues each located in one of the two IRA1 helices (Trp-775 in H1 and Phe-811 in H2). A third residue, Tyr-803, of H2 further "fixes" the IRA1 hairpin to SD by interacting with both H1 and SD. These residues fit into "sockets" formed by hydrophobic SD residues. Mutation of either one residue weakens SD binding to the DEAD motor (Fig. 3*B*; data not shown). (b) The second contact is IRA1-SSD; although SSD is separated from IRA1 by a large cavity (Fig. 5*B*) (18), defined contacts between IRA1 and the SSD bulb and $stem_{in}$ occur (18, 19). E806A and R792A mutations generated here are expected to interfere with IRA1-SSD bulb interaction. The inevitable consequence of such positioning is that IRA1 hairpin becomes the only physical link between the two "lever-like" appendages SSD and SD (Fig. 5, *A* and *B*) (18, 19), each rooted in one of the two DEAD motor subdomains (Fig. 1*A*). By binding to both SD and SSD (18, 19) and affecting their conformation (Figs. 2 (*A–D*) and 4*A*), IRA1 is appropriately placed to "manipulate" DEAD motor conformation and catalysis at a distance. This is achieved through a dynamic network of reciprocal conformational cross-talk (Fig. 2; Table II) (16, 17) that allows communication between the DEAD motor and its "specificity" appendages (SSD and C-domain).

The SD-IRA1-SSD interface bears the hallmarks of a coupling device that is dynamic. Although SD is the sole DEAD motor-binding determinant on the C-domain (18, 19), C-domain/DEAD motor binding requires the presence of IRA1 (Fig. 3*D*). Presumably, by binding to it IRA1 maintains SD in a conformation that possesses the characteristic bent (Fig. 5*A*) and is competent for DEAD motor association. W775A and F811A, which weaken IRA1 binding to SD (Fig. 5, *A* and *B*), also weaken C-domain binding to the DEAD motor (Fig. 3*A*, *lane 6*). Importantly, SD-mediated C-domain binding to the DEAD motor (Fig. 3*A*) determines DEAD motor ligand affinities (Table II; Fig. 1, *E* and *F*) and turnover (Table I). Thus, these "gain of function" mutations hyperactivate SecA ATPase in the absence of any translocation ligands. ATP catalysis by the F_1 ATPase β subunit is similarly regulated by binding and release of the elongated α-helical γ subunit (39). Interestingly, Trp-775 is mobile and moves in and out of its hydrophobic environment upon ligand binding to SecA (18, 26, 27, 34, 35). Shortening of the Trp side chain in W775A presumably mimics a state of IRA1 that is detached from SD. In contrast, W775F and W775Y mutations that retain bulky hydrophobic side

chains have practically wild type behavior (18, 34, 35).[2] We therefore anticipate that IRA1 "oscillates" laterally to and from SD throughout protein translocation. Taking into account the physical proximity of SSD to IRA1 (Fig. 5, *A* and *B*) and the effects of IRA1 mutations on SSD conformation (Fig. 2, *A–D*) and function (Fig. 1*E*), we expect that IRA1 may also bind and release from SSD during catalysis. Thus, IRA1 mutations may exert a general influence on plasticity of the SD-IRA1-SSD interface.

Taken together our data allow us to formulate the following working hypothesis: ATP-driven DEAD motor translocation work is conformationally coupled to cycles of SD association/dissociation, which in turn are coupled to cycles of IRA1 binding and release from SD, and these may be further coupled to cycles of IRA1 binding and release from SSD. We anticipate that these events are regulated by preprotein binding to SSD (17, 23) and SecYEG binding to the DEAD motor (Fig. 1*E*), both interactions affected by IRA1. Thus, IRA1 acts as a molecular switch (15) that "senses" translocation ligands, controls SecA conformational plasticity and subactivities. These properties render IRA1 a global co-ordinator of SecA and protein translocase catalysis.

Acknowledgments—We are grateful to K. Tokatlidis, A. Kuhn, and P. Soultanas for comments; A. Kuhn for use of equipment; Y. Papanikolau for help with software; and A. Driessen for plasmids.

REFERENCES

1. Driessen, A. J., Manting, E. H. & van der Does, C. (2001) *Nat. Struct. Biol.* **8,** 492–498
2. Economou, A. (2002) *Mol. Membr. Biol.* **19,** 159–169
3. Manting, E. H., van Der Does, C., Remigy, H., Engel, A. & Driessen, A. J. (2000) *EMBO J.* **19,** 852–861
4. Breyton, C., Haase, W., Rapoport, T. A., Kuhlbrandt, W. & Collinson, I. (2002) *Nature* **418,** 662–625
5. Hartl, F. U., Lecker, S., Schiebel, E., Hendrick, J. P. & Wickner, W. (1990) *Cell* **63,** 269–279
6. Brundage, L., Hendrick, J. P., Schiebel, E., Driessen, A. J. & Wickner, W. (1990) *Cell* **62,** 649–657
7. Douville, K., Price, A., Eichler, J., Economou, A. & Wickner, W. (1995) *J. Biol. Chem.* **270,** 20106–20111
8. Duong, F. & Wickner, W. (1997) *EMBO J.* **16,** 2756–2768
9. Duong, F. & Wickner, W. (1997) *EMBO J.* **16,** 4871–4879
10. Lill, R., Dowhan, W. & Wickner, W. (1990) *Cell* **60,** 271–280
11. Economou, A. & Wickner, W. (1994) *Cell* **78,** 835–843
12. Economou, A., Pogliano, J. P., Beckwith, J., Oliver, D. B. & Wickner, W. (1995) *Cell* **83,** 1171–1181
13. Economou, A. (1998) *Mol. Microbiol.* **27,** 511–518
14. Schiebel, E., Driessen, A. J. M., Hartl, F. U. & Wickner, W. (1991) *Cell* **64,** 927–939
15. Karamanou, S., Vrontou, E., Sianidis, G., Baud, C., Roos, T., Kuhn, A., Politou, A. S. & Economou, A. (1999) *Mol. Microbiol.* **34,** 1133–1145
16. Sianidis, G., Karamanou, S., Vrontou, E., Boulias, K., Rapanas, K., Kyrpides, N., Politou, A. S. & Economou, A. (2001) *EMBO J.* ***20,*** **5,** 961–970
17. Baud, C., Karamanou, S., Sianidis, G., Vrontou, E., Politou, A. S. & Economou, A. (2002) *J. Biol. Chem.* **277,** 13724–13731
18. Hunt, J. F., Weinkauf, S., Henry, L., Fak, J. J., McNicholas, P., Oliver, D. B. & Deisenhofer, J. (2002) *Science* **297,** 2018–2026
19. Sharma, V., Arockiasamy, A., Ronning, D. R., Savva, C. G., Holzenburg, A., Braunstein, M., Jacobs, W. R., Jr. & Sacchettini, J. C. (2003) *Proc. Natl. Acad. Sci. U. S. A.* **100,** 2243–2248
20. Caruthers, J. M. & McKay, D. B. (2002) *Curr. Opin. Struct. Biol.* **12,** 123–133
21. Delagoutte, E. & von Hippel, P. H. (2002) *Q. Rev. Biophys.* **35,** 431–478
22. Koonin, E. V. & Gorbalenya, A. E. (1992) *FEBS Lett.* **298,** 6–8
23. Kimura, E., Akita, M., Matsuyama, S. I. & Mizushima, S. (1991) *J. Biol. Chem.* **206,** 6600–6606
24. Kourtz, L. & Oliver, D. (2000) *Mol. Microbiol.* **37,** 1342–1356
25. Hirano, M., Matsuyama, S. & Tokuda, H. (1996) *Biochem. Biophys. Res. Commun.*, **229,** 90–95
26. Breukink, E., Nouwen, N., van Raalte, A., Mizushima, S., Tommassen, J. & de Kruijff, B. (1995) *J. Biol. Chem.* **270,** 7902–7907
27. Fekkes, P., de Wit, J. G., van der Wolk, J. P., Kimsey, H. H., Kumamoto, C. A. & Driessen, A. J. (1998) *Mol. Microbiol.* **29,** 1179–1190
28. Singleton, M. R. & Wigley, D. B. (2003) *EMBO J.* **22,** 4579–4583
29. Mitchell, C. & Oliver, D. (1993) *Mol. Microbiol.* **10,** 483–497
30. Jarosik, G. P. & Oliver, D. B. (1991) *J. Bacteriol.* **173,** 860–868
31. den Blaauwen, T., van der Wolk, J. P., van der Does, C., van Wely, K. H. & Driessen, A. J. (1999) *FEBS Lett.* **458,** 145–150
32. Dapic, V. & Oliver, D. (2000) *J. Biol. Chem.* **275,** 25000–25007
33. Miller, A., Wang, L. & Kendall, D. A. (1998) *J. Biol. Chem.* **273,** 11409–11412
34. Ding, H., Mukerji, I. & Oliver, D. (2001) *Biochemistry* **40,** 1835–1843
35. den Blaauwen, T., Fekkes, P., de Wit, J. G., Kuiper, W. & Driessen, A. J. (1996) *Biochemistry* **35,** 11194–12004
36. Triplett, T. L., Sgrignoli, A. R., Gao, F. B., Yang, Y. B., Tai, P. C. & Gierasch, L. M. (2001) *J. Biol. Chem.* **276,** 19648–19655
37. Yap, K. L., Ames, J. B., Swindells, M. B. & Ikura, M. (1999) *Proteins* **37,** 499–507
38. Song, M. & Kim, H. (1997) *J. Biochem.* (*Tokyo*) **122,** 1010–1018
39. Yoshida, M., Muneyuki, E. & Hisabori, T. (2001) *Nat. Rev. Mol. Cell Biol.* **2,** 669–677

[2] G. Sianidis and A. Economou, unpublished results.